https://doi.org/10.5194/soil-2020-44
Preprint. Discussion started: 23 July 2020

SOIL Discussions Open Access EGU

Oxygen isotope exchange between water and carbon dioxide in soils is controlled by pH, nitrate availability and microbial biomass through links to carbonic anhydrase activity

Sam P. Jones[1,2], Aurore Kaisermann[1], Jerome Ogee[1], Steven Wohl[1], Alexander W. Cheesman[3], Lucas A. Cernusak[3], and Lisa Wingate[1]

[1] INRA, UMR ISPA, 33140, Villenave d'Ornon, France
[2] Instituto Nacional de Pesquisas da Amazônia, Manaus – AM, CEP 69060-001, Brasil
[3] College of Science and Engineering, James Cook University, Cairns, Queensland, Australia

Correspondence to: Sam P. Jones (sam.p.jones@hotmail.co.uk)

Abstract. The oxygen isotope composition ($\delta^{18}O$) of atmospheric carbon dioxide (CO_2) can be used to estimate gross primary production at the ecosystem-scale and above. Understanding how and why the rate of oxygen isotope exchange between soil water and CO_2 (k_{iso}) varies can help to reduce uncertainty in the retrieval of such estimates. The expression and activity of carbonic anhydrases in soils are important drivers of variations in k_{iso}. Here we estimate k_{iso} and measure associated soil properties in laboratory incubation experiments using 44 soils sampled from sites across western Eurasia and northeastern Australia. Observed k_{iso} exceeded theoretical uncatalysed rates indicating the significant influence of carbonic anhydrases on the variability observed among the soils studied. We identify soil pH as the principal source of variation, with greater k_{iso} under alkaline conditions suggesting that shifts in microbial community composition or intra-extra cellular dissolved inorganic carbon gradients induce the expression of more or higher activity forms of carbonic anhydrases. We also show for the first time in soils that the presence of nitrate under acidic conditions reduces k_{iso}, potentially reflecting the direct or indirect inhibition of carbonic anhydrases. This effect was confirmed by a supplementary ammonium nitrate fertilisation experiment conducted on a subset of the soils. Future changes in atmospheric nitrogen deposition or land-use may thus influence carbonic anhydrase activity. Greater microbial biomass also increased k_{iso} under a given set of chemical conditions likely highlighting the ubiquity of carbonic anhydrase expression by soil microbial communities. These data provide the most extensive analysis of spatial variations in soil k_{iso} to date and indicate key controls required to predict variations in k_{iso} at the scales needed to improve efforts to constrain gross primary productivity using the $\delta^{18}O$ of atmospheric CO_2.

https://doi.org/10.5194/soil-2020-44
Preprint. Discussion started: 23 July 2020

1 Introduction

The rate of oxygen isotope exchange (k_{iso}) between soil water and carbon dioxide (CO_2) is a key uncertainty in estimating the gross contribution of terrestrial uptake and release to net land-atmosphere carbon exchange from the oxygen isotope composition ($\delta^{18}O$) of atmospheric CO_2 (Wingate et al., 2009; Welp et al. 2011). The $\delta^{18}O$ of atmospheric CO_2 can be used to trace these large and opposing fluxes because the $\delta^{18}O$ of leaf-atmosphere CO_2 exchange tends to be enriched and distinct compared to well mixed atmospheric CO_2 and thus has the potential to serve as an independent tracer of gross primary production (Francey & Tans, 1987). This is the case because the leaves of plants contain considerable concentrations of carbonic anhydrases, which catalyse the hydration of aqueous CO_2 and in turn the exchange of oxygen isotopes with water molecules, causing CO_2 that interacts with a leaf but is not fixed to inherit the isotopic composition of the leaf water pool (Gillon & Yakir, 2001). As leaf water pools are small and undergo considerable enrichment during evaporation the $\delta^{18}O$ of this water is enriched relative to that of the soil water and thus CO_2 that has interacted with leaves has a distinct isotopic signature in the atmosphere (Francey & Tans, 1987). However, the presence of carbonic anhydrases is not limited to leaves with a number of forms also found in soils (Meredith et al., 2019), but the abundance and activity of these enzymes is poorly known and the degree to which their influence on k_{iso} alters the $\delta^{18}O$ of atmospheric CO_2 is not well constrained. As such, improved understanding of variations in soil k_{iso} benefits efforts to constrain variability and controls on carbon exchange at the ecosystem-level and above.

Comprising at least six distinct families, carbonic anhydrases have independently evolved in all domains of life in order to catalyse the reversible hydration of carbon dioxide (CO_2) to bicarbonate (Del Prete et al., 2014). Whilst this reaction occurs abiotically, the need for carbonic anhydrases stems from the fact that enhanced rates of hydration, k_h (s^{-1}), are required to control the transport and availability of CO_2, bicarbonate and protons in numerous metabolic processes (Smith & Ferry, 2000). Unsurprisingly given their apparent ubiquity, evidence of carbonic anhydrase activity in soils indicates the expression of these enzymes directly supports the viability of microbial communities and thus plays a role in the wider biogeochemical function of the soil environment (Li et al., 2005). An indirect consequence of increased rate of hydration, k_h, associated with the presence of these enzymes is that it also influences the oxygen isotope composition ($\delta^{18}O$) of atmospheric CO_2. The $\delta^{18}O$ of atmospheric CO_2 is influenced by carbonic anhydrases because oxygen isotopes are exchanged between water and CO_2 through the reverse dehydration reaction (Mills & Urey, 1940). In a closed system at chemical equilibrium, CO_2 will reach isotopic equilibrium with water after some time depending on the rate, k_{iso} (s^{-1}), of oxygen isotope exchange (Uchikawa & Zeebe, 2012). In soils the greater abundance of water molecules means that endogeneous CO_2 or atmospheric CO_2 that abiotically invades the soil tends to inherit the $\delta^{18}O$ of the soil water (Tans, 1998). The degree to which the $\delta^{18}O$ of CO_2 reflects a given soil water pool is determined by the residence time of dissolved CO_2 and the apparent k_{iso} (Miller et al.,

https://doi.org/10.5194/soil-2020-44
Preprint. Discussion started: 23 July 2020

1999). Longer residence times or greater k_{iso} move the system closer to isotopic equilibrium. Resulting from the interconversion of aqueous CO_2 and bicarbonate, k_{iso} is expected to vary as a function of the combined rates of CO_2 hydration, k_h, and hydroxylation reactions and the pH dependent speciation of dissolved inorganic carbon (Uchikawa & Zeebe, 2012). Under acidic and neutral conditions interconversion is dominated by hydration, whilst the hydroxylation becomes important under alkaline conditions as the concentration of hydroxyl anions increases (Figure 1 a). The presence of carbonic anhydrases increases the rate of the hydration reaction and the overall rate of interconversion. However, the influence of carbonic anhydrases, for a given concentration and efficiency, is also limited by the presence of high proton concentrations under acidic conditions that inhibit de-protonation required for enzyme regeneration (Rowlett et al., 2002; Sauze et al., 2018). The k_{iso} resulting from these reactions is dependent on the relative abundance of CO_2, which is only the dominant form of dissolved organic carbon under acidic conditions, to true carbonic acid, bicarbonate and carbonate in the system (Figure 1 b). In alkaline conditions, the predominance of bicarbonate and carbonate acts to inhibit the rate of k_{iso} associated with the hydration reaction and limit the influence of hydroxylation (Figure 1 c). The fact that k_{iso} inferred from patterns in $\delta^{18}O$ of CO_2 fluxes observed under field (Seibt et al., 2006; Wingate et al., 2008, 2009, 2010) and laboratory conditions (Jones et al., 2017; Meredith et al., 2019; Sauze et al., 2017, 2018) can exceed uncatalysed rates predicted by this theoretical basis by up to three orders of magnitude indicates a particular need to better understand variations in the expression of carbonic anhydrases and the controls on their activity in soil environments.

The ubiquity of carbonic anhydrases expression by organisms (Smith & Ferry, 2000) has been invoked to explain variations in the rate, k_h, of hydration (Li et al., 2005) and the rate, k_{iso}, of oxygen isotope exchange (Wingate et al., 2009) in soils as a function of the size and composition of the microbial communities present. That is to say if carbonic anhydrase expression is widespread within a microbial community or a specific functional group, increases in their abundance will result in greater concentrations of carbonic anhydrases within the soil and thus greater reaction rates. Indeed, such a driver for k_{iso} is supported by experimental observations showing that rates increase with algae (Sauze et al., 2017) and α- and β-carbonic anhydrase (Meredith et al., 2019) abundances. Whilst the sensitivity of soil k_{iso} to the presence of specific functional groups, like phototrophs which employ carbonic anhydrases in their carbon concentration mechanisms (Badger, 2003), is clear from these studies, the influence of wider community size and composition and it's utility in predicting variations remains uncertain. Soil k_{iso} has also been shown to vary in response to soil pH, with greater rates under alkaline conditions (Sauze et al., 2018). The observed increase, contrary to the decrease (Figure 1 c) that would be expected to be induced by the shift in dissolved inorganic carbon speciation (Figure 1 b) at a constant carbonic anhydrase concentration and efficiency (Figure 1 a), suggests a greater abundance or the presence of more efficient forms of carbonic anhydrases at higher soil pH. Such an observation may result from changes in size or composition of the microbial communities involved as discussed (Sauze et al., 2017, 2018). Alternatively this pattern might be driven by the up-regulation of carbonic anhydrase expression by organisms, which tend to maintain more neutral conditions than their environment (Krulwich et al., 2011), in order to control

https://doi.org/10.5194/soil-2020-44
Preprint. Discussion started: 23 July 2020

intra-extra cellular dissolved inorganic carbon gradients (Smith & Ferry, 2000) in response to changes in extra-cellular CO_2 and bicarbonate availability (Figure 1 b). Such a control may be supported by the fact both bacteria and fungi grown under CO_2 limited conditions have been shown to increase the expression of carbonic anhydrases (Kaur et al., 2009; Kozliak et al., 1995; Merlin et al., 2003). Indeed, such a response in order to maintain the supply of CO_2 in bicarbonate dominated systems has been documented for aquatic phototrophs (Hopkinson et al., 2013). The chemistry of non-carbon anions may also play a role in controlling the activity of carbonic anhydrases (Tibell et al., 1984) with the presence of phosphate for example potentially inhibiting extra-cellular carbonic anhydrase activity in soil solutions and thus decreasing k_{iso} (Sauze et al., 2018). In this respect, the fact that nitrate (NO_3^-) has been shown to inhibit carbonic anhydrases (Peltier et al., 1995) suggests that the inorganic nitrogen chemistry of soil solutions may exert a control, particularly in the context of fertilised agriculture soils or increased atmospheric nitrogen deposition. Indeed, the inhibition of soil carbonic anhyrases by nitrogen fertilisation has been inferred from measurements of carbonyl sulphide exchange (Kaisermann et al., 2018b), but the influence on k_{iso} has yet to be considered.

Here we investigate variations in the rate of oxygen isotope exchange, k_{iso}, through controlled laboratory gas exchange measurements on soil incubations. To understand the drivers of these variations we measured soils, with different chemical and physical properties, sampled from 44 sites across western Eurasia and northeastern Australia. We also conducted a fertilisation experiment on a subset of these soils to investigate the influence of changes in nitrogen availability. We tested three specific, non-exclusive, hypotheses; 1) k_{iso} increases with increases in microbial biomass reflecting the common nature of carbonic anhydrase expression by soil organisms (H1), 2) k_{iso} increases with increases in soil pH reflecting an increase in the amount or efficiency of expressed carbonic anhydrases either because of the response of organisms to unfavourable gradients in intra-extra cellular dissolved inorganic carbon under alkaline conditions or a shift in active functional groups (H2), and 3) k_{iso} will decrease with increases in NO_3^- availability as it binds with carbonic anhydrases and directly inhibits enzymatic activity (H3). For the Eurasian soils we also compare these drivers to the predictive power of relatively invariant soil properties that might be used to estimate the rate of exchange in soils at the regional scale and above as required by efforts to better constrain gross primary production.

2 Methods

To investigate the outlined hypotheses two similar measurement campaigns, each consisting of a spatial survey and an ammonium nitrate (NH_4NO_3) addition experiment, were conducted aimed at characterising the controls on variations in the rate of oxygen isotope exchange, k_{iso}, across soils from a wide range of environments. In both cases we estimated k_{iso} from gas exchange and soil physical property measurements (Jones et al., 2017; Sauze et al., 2018) and subsequently measured the pH, microbial biomass, NO_3^- availability and NH_4^+ availability of the incubated soils to investigate the controls on this

https://doi.org/10.5194/soil-2020-44
Preprint. Discussion started: 23 July 2020

activity. The first campaign focused on soils sampled from across western Eurasia (EUR) whilst the second (AUS) focused on soils sampled in north Queensland, Australia. Sampling sites were broadly classified based on the principle land-cover reported by previous studies or observed during sampling and climatic zone as indicted by the Köppen-Geiger climate classification map of Kottek et al., (2006) and Rubel et al., (2017).

2.1 Soil sampling and incubation preparation

For the EUR campaign, collaborators (see acknowledgements) sampled the superficial 10 cm of soil at three locations within 27 sites during the Northern hemisphere summer of 2016 and shipped the soil samples to the Bordeaux-Aquitaine Center of the National Institute of Agricultural Research, France (Figure S1 a). These sites fell within Subarctic (Dfc; n= 6), Temperate oceanic (Cfb; n= 13), Hot-summer Mediterranean (Csa; n = 7) and Hot semi-arid (Bsh; n = 1) climate zones and were principally found in forests (n = 16) and grasslands (n = 6). The other remaining sites were located in an agricultural field (n = 1), a peatland (n = 1) and orchards (n = 3). Upon receipt, samples were passed through a 4 mm sieve and mixed to create one homogeneous sample for each site. These soils were stored at 4 °C. A sub-sample of each of these soils was used to determine the initial water content and the soil water holding capacity (Haney & Haney, 2010). For each soil three replicate incubations were prepared with glass jars of 15.54 cm in height and an internal diameter of 8.74 cm. A jar was filled with the wet weight equivalent of 115 to 300 g of dry soil and the water content adjusted to 30 % of the water holding capacity to create a soil column with a surface area of 60.0 cm^2 and a depth of approximately 4 to 7 cm. The jar was then pre-incubated in a climate-controlled cabinet (MD1400, Snijders, Tillburg, NL) for two weeks in the dark at 22 ± 1 °C. This cabinet was continuously flushed with approximately 20 L min^{-1} of ambient air provided by a pump with an inlet outside of the building to avoid exposing the soil to elevated CO_2 concentrations found within the laboratory. During this period, soil water content was periodically adjusted to account for evaporation. Approximately 18 hours prior to measurement the jar was closed with a screw-tight glass lid equipped with inlet and outlet connections and flushed at 250 mL min^{-1} with dry, synthetic air to promote steady-state conditions. This flow was produced using an in-house dilution system that mixed pure CO_2 from a cylinder into CO_2-free air generated by an air compressor (FM2 Atlas Copto, Nacka, Sweden) equipped with a scrubbing column (Ecodry K-MT6, Parker Hannifin, USA). This system was set to achieve a CO_2 concentration of 400 ± 5 ppm and, reflecting the origin of the CO_2 in the cylinder used, had a $\delta^{18}O$ of approximately −25 ‰ $VPDB_g$. Subsequently the jar was removed to conduct gas exchange and soil property measurements.

For the AUS campaign, we sampled the superficial 10 cm of soil at four locations within 17 sites during July of 2017 and returned these samples to the Cairns campus of James Cook University (Figure S1 b). These sites fell within Tropical monsoon (Am; n = 3), Humid subtropical (Cfa; n = 9) and Monsoon-influenced humid subtropical (Cwa; n= 5) climate zones and were principally found in forests (n = 9) and savannas (n = 6), with the other remaining sites located in a pasture

https://doi.org/10.5194/soil-2020-44
Preprint. Discussion started: 23 July 2020

(n = 1) and a stunted shrub-rich forest (n = 1). These soils were passed through a 4 mm sieve and mixed to create a homogenous sample for each site. A sub-sample of each of these soils was used to determine the initial water content and estimate the re-packed bulk density of the soils. As with the EUR campaign, three replicate incubations were prepared in glass jars for each soil. These jars had a height of 11.56 cm and an internal diameter of 7.45 cm. A jar was filled with the wet weight equivalent of 215 to 450 g of dry soil and the water content adjusted to 30 % water-filled pore space to create a soil column with a surface area of 43.5 cm^2 and a depth of approximately 8.5 cm. The jar was then pre-incubated in an insulated box for one week in the dark at 23 ± 1 °C with periodic adjustments to the water content to account for evaporation. This box was continuously flushed with approximately 10 L min^{-1} of ambient air provided by an air compressor that serviced building wide laboratory air distribution. The concentration of CO_2 in this air was approximately 420 ppm and, and reflecting it's atmospheric origin, had a $\delta^{18}O$ of approximately 0 ‰ $VPDB_g$. Following pre-incubation the jar was removed to conduct gas exchange and soil property measurements.

An NH_4NO_3 addition experiment was conducted in both campaigns. To do so an additional three replica incubations were prepared as described above, with these untreated soils serving as controls, for nine and five soils of the EUR and AUS campaigns respectively. Prior to the pre-incubation step, 0.7 mg of NH_4NO_3 g dry $soil^{-1}$ was added dissolved in the water used to adjust the water content. This quantity was chosen following Ramirez et al., (2012) to approximate a treatment comparable to typical field studies.

2.1 Gas exchange measurements

Gas exchange measurements were made using a similar experimental set-up to that described in Jones et al., (2017). Each jar was connected to a gas delivery system that supplied one of two gas sources, $\delta_{b,atm}$ or $\delta_{b,mix}$, to its inlet. The first inlet condition, $\delta_{b,atm}$, consisted of a continuous flow of atmospheric air pumped from an external buffer volume, through a Drierite column (W. A. Hammond DRIERITE Co. LTD, USA) to dry the air and directly to the inlet of the jar. The second condition, $\delta_{b,mix}$, was produced by a second continuous flow of atmospheric air pumped from the buffer, through a soda lime column to remove CO_2 and a second Drierite column. A mass-flow controller was used to dilute pure CO_2 from a cylinder into this dry CO_2 free air and then this mix was supplied to the inlet of the jar. The flow rate of pure CO_2 was controlled to match the concentration of the CO_2 in $\delta_{b,mix}$ to that of $\delta_{b,atm}$ using a control loop feedback based on the difference in concentration between sub-samples of both flows measured with an infra-red CO_2 analyser (Li-6262, LI-COR Biosciences, USA). By doing so the principal difference between the two conditions was the isotopic composition of the CO_2 present reflecting its origin in the atmosphere ($\delta^{18}O$-CO_2 of $\delta_{b,atm}$ = −1.41 ± 2.17 ‰ $VPDB_g$) or a cylinder ($\delta^{18}O$-CO_2 of $\delta_{b,mix}$ = −25.33 ± 0.30 ‰ $VPDB_g$). The delivery of either gas to the inlet of the jar was operated by a valve manifold and micro-

https://doi.org/10.5194/soil-2020-44
Preprint. Discussion started: 23 July 2020

controller. Following the manifold, the selected gas stream was split into a chamber line, to which the jar was connected, and a bypass line that terminated at open splits in front of a valve connected to the sample inlet of a CO_2 isotope ratio infrared spectrometer (Delta Ray IRIS, Thermo Fischer Scientific, Germany). The flow rate of the chamber line was limited to 171.48 μmol s^{-1} using a mass-flow controller. The micro-controller was set to supply first one inlet condition through the manifold to the chamber and bypass line and then switch to the second inlet condition. Both inlet conditions were supplied for either 32 (EUR) or 34 (AUS) minutes. The first 20 (EUR) or 22 (AUS) minutes under each condition were used to flush the system and promote steady-state conditions in the incubation jar. After this period, the final 12 minutes during which the condition was supplied before switching was used for gas-exchange measurements. During this 12 minute measurement period the valve in front of the IRIS switched three times between the chamber and bypass line at two minute intervals. Calibration gas was measured every 16 (EUR) or 18 (AUS) minutes with sequential two minute measurements of two cylinders containing synthetic air with different CO_2 concentrations but similar isotopic compositions. The concentrations of $^{12}C^{16}O^{16}O$, $^{13}C^{16}O^{16}O$ and $^{12}C^{18}O^{16}O$ recorded by the IRIS were processed as described in detail by Jones et al. (2017) to average the final 40 s of data collected for each two minute interval discussed and calculate corrected concentrations and isotope ratios.

Reflecting the pre-incubation conditions, measurements for EUR began with $\delta_{b,mix}$ as the inlet condition before switching to $\delta_{b,atm}$, whilst for AUS the sequence began with $\delta_{b,atm}$ and then switched to $\delta_{b,mix}$. For EUR, the calibration cylinders (21 % O_2 and 0.93 % Ar in a N_2 balance, Deuste Steinger GmbH, Germany) had total concentration, carbon isotope composition and $\delta^{18}O$ of CO_2, respectively, of 380.26 ppm , −3.06 ‰ VPDB, and −14.63 ‰ $VPDB_g$ for the first cylinder, and 481.62 ppm , −3.07 ‰ VPDB and 14.70 ‰ $VPDB_g$ for the second cylinder (IsoLab, Max Planck Institute for Biogeochemistry, Germany). For AUS, the calibration cylinders (21 % O_2 and 1.12 % Ar in a N_2 balance, BOC, Australia) had total concentration, carbon isotope composition and $\delta^{18}O$ of CO_2, respectively, of 386.7 ppm, −33.42 ‰ VPDB and −26.33 ‰ $VPDB_g$, for the first cylinder, and 486.7 ppm, −33.64 ‰ VPDB and −26.60 ‰ $VPDB_g$ for the second cylinder (Farquhar Laboratory, Australian National University, Australia).

The net CO_2 flux, F_R (μmol m^{-2} s^{-1}), was calculated from corrected values for the three pairs of chamber and bypass line measurements made at each inlet condition following Eq. (1):

$$F_R = \frac{u}{A}\left(C_c - C_b\right), \quad (1)$$

where u is the flow rate (mol m^{-3} s^{-1}) through the chamber line, C_c is the total CO_2 concentration (ppm) of the chamber line, C_b is the total CO_2 concentration (ppm) of the bypass line and A is the surface area (m^2) of the soil in the chamber. The resultant three values for each inlet condition were then averaged to yield a single flux rate. Similarly the $\delta^{18}O$ of CO_2 exchange, δ_R (‰ $VPDB_g$), was calculated following Eq. (2):

https://doi.org/10.5194/soil-2020-44
Preprint. Discussion started: 23 July 2020

$$\delta_R = \frac{\left(\delta_c C_{c,12} - \delta_b C_{b,12}\right)}{\left(C_{c,12} - C_{b,12}\right)}, \quad (2)$$

where δ_c is the $\delta^{18}O$ of CO_2 (‰ $VPDB_g$) in the chamber line, δ_b is the $\delta^{18}O$ of CO_2 (‰ $VPDB_g$) in the bypass line, $C_{c,12}$ (ppm) is the concentration of $^{12}C^{16}O^{16}O$ in the chamber line and $C_{b,12}$ (ppm) is the concentration of $^{12}C^{16}O^{16}O$ in the bypass line.

2.3 Soil properties

After being disconnected from the gas exchange system, a jar was weighed to determine the wet weight of the incubated soil and the total soil depth, z_{max} (m), measured using a caliper. Soil was then removed from the jar to determine soil water content, pH, microbial biomass, NO_3^- availability and NH_4^+ availability. Soil water contents were determined gravimetrically for sub-samples based on water loss after oven drying for 24 hours at 105 °C. In the EUR campaign, soil water content was determined for three, 1.5 cm thick intervals between 0.0 and 4.5 cm depth. An average gravimetric water content (g g dry $soil^{-1}$) was calculated for the soil column after weighting by total soil depth. In the AUS campaign, soil water content was determined for a single sample covering the total soil depth. Soil bulk density (g cm^{-3}) was calculated from the gravimetric water content, the wet weight of the soil in the jar and the volume of the soil column. Total porosity, ϕ_t, was calculated from bulk density assuming a particle density of 2.65 g cm^{-3} (Linn & Doran, 1984). Volumetric water content, θ_w (m^3 m^{-3}), was calculated as the product of gravimetric water content and bulk density. The soil air-filled porosity, ϕ_a, was calculated as the difference between the total porosity and volumetric water content. The remaining soil column in the jar was then mixed and sub-samples were taken to determine pH, microbial biomass, NO_3^- availability and NH_4^+ availability. Soil pH was determined in a slurry with a dry weight equivalent soil-to-water ratio of 1:5. Soil microbial biomass (µg C g dry $soil^{-1}$) was determined based on the difference between dissolved carbon extracted from non-fumigated and chloroform-fumigated sub-samples using a slurry with a dry weight equivalent soil-to-potassium sulphate solution (0.5 M) ratio of 1:5 and an extraction efficiency value of 0.35. Available NO_3^- (µg N g dry $soil^{-1}$) and NH_4^+ (µg N g dry $soil^{-1}$) were extracted in a slurry with a dry weight equivalent soil-to-potassium chloride solution (1 M) ratio of 1:5. These extracts were filtered, frozen at −20 °C and shipped on dry ice to commercial laboratories (EUR: LAS INRA Hauts-de-France, Arras, France; AUS: ASL Environmental, Brisbane, Queensland, Australia) for determination of dissolved carbon, NO_3^- and NH_4^+ concentrations. Sub-samples of the homogenised soil used to fill jars in the EUR campaign were also taken to determine soil texture and carbon, nitrogen and carbonate content by sampling site as part of a related study (Kaisermann et al., 2018a).

https://doi.org/10.5194/soil-2020-44
Preprint. Discussion started: 23 July 2020

2.4 Estimating the oxygen isotope exchange rate

Following Jones et al., (2017) the rate of oxygen isotope exchange between soil water and CO_2, k_{iso}, was estimated from the inverse of the slope of the linear relationship between the $\delta^{18}O$ of CO_2 exchange and the $\delta^{18}O$ of CO_2 at the soil surface. Briefly, under the two gas-exchange measurement conditions induced by varying the $\delta^{18}O$ of CO_2 at the incubation inlet ($\delta_{b,mix}$ and $\delta_{b,atm}$), the invasion flux or piston velocity of CO_2, v_{inv} (m s^{-1}), can be estimated following Eq. (3):

$$v_{\mathrm{inv}} = \frac{F_{\mathrm{R},\mu}}{C_{\mathrm{a},\mu}} \frac{\left(\delta_{\mathrm{R,mix}} - \delta_{\mathrm{R,atm}}\right)}{\left(\delta_{\mathrm{a,atm}} - \delta_{\mathrm{a,mix}}\right)} \quad , \tag{3}$$

where δ_R (‰ $VPDB_g$) is the $\delta^{18}O$ of CO_2 exchange and δ_a (‰ $VPDB_g$) is the $\delta^{18}O$ of CO_2 at the soil surface under the two different inlet conditions ($\delta_{b,mix}$ and $\delta_{b,atm}$) and $F_{R,\mu}$ (μmol m^{-2} s^{-1}) is the mean net CO_2 flux under both conditions and $C_{a,\mu}$ (μmol m^{-3}) is the mean total CO_2 concentration at the soil surface measured under both conditions. Both δ_a and C_a were assumed equal to the δ_c and C_c measured in the chamber line as discussed previously. To correct for the influence of boundary conditions found at the bottom of incubation jars, particularly in shallower soil columns, the soil-depth adjusted invasion flux, $\tilde{v}_{inv}$ (m s^{-1}), was determined iteratively to satisfy Eq. (4):

$$0 = \tilde{v}_{\mathrm{inv}} \tanh\left(\frac{\tilde{v}_{\mathrm{inv}} z_{\max}}{\kappa \phi_a D}\right) - v_{\mathrm{inv}} \quad , \tag{4}$$

where z_{max} (m) is the total soil-column depth, κ is soil tortuosity calculated here following the formulation of Moldrup et al. (2003) for repacked soils, D (m^2 s^{-1}) is the diffusivity of $^{12}C^{16}O^{18}O$ in air (Massman, 1998; Tans, 1998) and ϕ_a is the air-filled porosity of the soil (see Sauze et al., (2018) for the derivation). Subsequently k_{iso} (s^{-1}) was calculated following Eq. (5):

$$k_{\mathrm{iso}} = \frac{\tilde{v}_{\mathrm{inv}^2}}{\kappa \phi_a \mathrm{DB} \theta_w} \quad , \tag{5}$$

where B (m^3 m^{-3}) is the Bunsen solubility coefficient for CO_2 in water (Weiss, 1974) and θ_w (m^3 m^{-3}) is the soil volumetric water content.

2.5 Statistical analyses

Statistical analyses were conducted in R version 3.5 (R Core Team, 2019). Of the 174 individual incubations prepared, 10 were excluded from the dataset because a record for one of the variables of interest; the rate, k_{iso}, of oxygen isotope exchange, pH, microbial biomass, NO_3^- availability or NH_4^+ availability, was missing. For the remaining 164 incubations

https://doi.org/10.5194/soil-2020-44
Preprint. Discussion started: 23 July 2020

with complete records, these variables were averaged by sampling site and, for the relevant subset, by whether they received a NH_4NO_3 addition.

The resultant dataset consisted of mean observations for 44 untreated soils (n = 27 / EUR and 17 / AUS) and 14 soils (n = 9 / EUR and 5 / AUS) that received a NH_4NO_3 addition. Spatial controls on k_{iso} were investigated across the means of untreated soils. Correlations between k_{iso}, pH, microbial biomass, NO_3^- availability and NH_4^+ availability were investigated through the Spearman's rank correlation between pairs of variables. To test the outlined hypotheses, a multiple generalised linear modelling approach was used to investigate which variables best explained variations in k_{iso} (Thomas et al., 2017). As pH and NH_4^+ availability were strongly negatively correlated (Spearman's $\rho = -0.73$), presumably reflecting the pH dependency of NH_4^+ and ammonia speciation, these were not considered together in the same model whilst all other possible combinations, including sampling campaign (EUR or AUS) to test for the undue influence of systematic experimental differences, were tested. Combinations were limited to models containing four or less predictive terms to prevent over-fitting and each independent variable was centered and scaled to facilitate comparison among the different measurement scales. The model structure and predictive terms included in the minimal adequate model required to explain variations in k_{iso} were selected based on comparison of sample size corrected Aikake's Information Criterion (AICc) and visual assessment of the conformity of model residuals to the assumptions of normality, homogeneity and the absence of unduly influential observations. This model was subsequently re-fitted with the original unstandardised variables. The same approach, limited to two-term models, was also applied to only the 27 soils from the EUR sampling campaign and extended to consider the relationships with soil texture and carbon and nitrogen contents to investigate their utility in upscaling efforts.

To investigate the influence of the NH_4NO_3 addition on the rate of oxygen isotope exchange, k_{iso}, the variables of interest were expressed as the ratio of the mean of the soils that received an addition and that of their respective untreated counterparts with quotients smaller and greater than one respectively indicating a reduction and increase following addition. Correlations between these fractional changes for k_{iso}, microbial biomass, pH, NO_3^- availability and NH_4^+ availability were investigated through the Spearman's rank correlation between pairs of variables. The minimal adequate, generalised linear model describing the fractional change in k_{iso} across these soils was investigated by comparing the AICc and visual inspection of the residuals for models that considered each independent variable separately to avoid over-fitting.

https://doi.org/10.5194/soil-2020-44
Preprint. Discussion started: 23 July 2020

3 Results

3.1 Variations among untreated soils

Clear differences in the rate, k_{iso}, of oxygen isotope exchange, pH, microbial biomass, NO_3^- availability and NH_4^+ availability were not apparent as a function of sampling site climatic zone or land-cover (Figure 2). Estimates of k_{iso} ranged from 0.01 to 0.40 s^{-1} with the greatest rates occurring in soils sampled from hot-summer Mediterranean (Csa) , hot semi-arid (Bsh) and subtropical (Cfa and Cwa) climates (Figure 2 a). Soil pH ranged from 3.9 to 8.6 and were mostly acidic or neutral with alkaline conditions only found for soils sampled from hot-summer Mediterranean (Csa) and hot semi-arid (Bsh) climates (Figure 2 b). Ranging from 98.5 to 2898.1 µg C g dry $soil^{-1}$, microbial biomass did not appear to vary systematically with sampling site origin. Available NO_3^- (Figure 2 d) ranged from 0.3 to 275.7 µg N g dry $soil^{-1}$ and available NH_4^+ (Figure 2 e) ranged from 2.5 to 64.7 µg N g dry $soil^{-1}$ with greatest availability found in soils sampled from temperate climates.

Individual relationships between pairs of these variables were investigated through Spearman's rank correlation (Table 1). Strong, significant correlations ($p < 0.05$) were only found between the rate of oxygen isotope exchange, k_{iso}, and soil pH (Spearman's $\rho = 0.58$), k_{iso} and NH_4^+ availability (Spearman's $\rho = -0.62$), and soil pH and NH_4^+ availability (Spearman's $\rho = -0.73$). Correlations between all other variable pairings were weaker and non-significant ($p > 0.05$).

Based on AICc and visual inspection of model fit and residuals, the structure of the generalised linear model describing variations in the rate of oxygen isotope exchange, k_{iso}, as the response variable was specified with a gaussian error distribution and log-link function (Thomas et al., 2017). The minimal adequate model with this structure (Figure S2) included the additive effects of soil pH (0.122), the natural logarithm of NO_3^- availability (−0.730) and the natural logarithm of microbial biomass (0.463), the interaction between soil pH and the natural logarithm of NO_3^- availability (0.109) and an intercept term (−6.046). This model explained 71 % of the deviance in k_{iso} (Figure 4 a) compared to the null model containing only an intercept term. The best model had an AICc that was 6.1 lower than the next best alternative model which omitted the interaction term, 7.1 lower than the closest model containing sampling campaign and 13.3 lower than the closest model containing the natural logarithm of NH_4^+ availability. The AICc values of single-term models containing only pH or the natural logarithms of microbial biomass or NO_3^- availability were respectively 21.6, 43.6, and 50.2 greater than the best model. The selected model predicts the response variable, $k_{iso\text{-}pred}$ (s^{-1}), in the original measurement units following Eq. (6):

$$\ln\left(k_{iso-pred}\right) = 0.122 \times pH - 0.730 \times \ln\left(NO_3^-\right) + 0.463 \times \ln\left(MB\right) + 0.109 \times pH \times \ln\left(NO_3^-\right) - 6.046 \quad , \quad (6)$$

https://doi.org/10.5194/soil-2020-44
Preprint. Discussion started: 23 July 2020

where pH is soil pH, NO_3^- is NO_3^- availability (μg N g dry $soil^{-1}$) and MB is microbial biomass (μg C g dry $soil^{-1}$). The model predicts that variations in k_{iso} result from positive correlations with soil pH (Figure 3 a) and microbial biomass (Figure 3 c) and negative correlation with NO_3^- availability. The interaction between soil pH and NO_3^- availability is such that the negative influence of NO_3^- on k_{iso} occurs mainly under acidic conditions and is marginal at neutral to alkaline pH (Figure 3 b).

As with the full dataset, across the 27 soils from the EUR sampling campaign the strongest relationship with the rate of oxygen isotope exchange, k_{iso}, was found with pH (Spearman's $\rho = 0.58$), whilst a weaker but still significant ($p < 0.05$) relationship with NO_3^- availability (Spearman's $\rho = -0.42$) was also identified. No significant ($p > 0.05$) relationships between k_{iso} and clay (Spearman's $\rho = 0.11$), silt (Spearman's $\rho = -0.18$), sand (Spearman's $\rho = 0.00$), carbon (Spearman's $\rho = -0.03$) or nitrogen (Spearman's $\rho = -0.32$) contents were found, whilst, the relationship with the ratio between total carbon and nitrogen content (Spearman's $\rho = 0.38$) was marginal ($p = 0.05$). The minimal adequate generalised linear model explaining variations in k_{iso} selected from only the relatively invariant properties of soil texture and carbon and nitrogen content included only the intercept (−2.128) and the effect of nitrogen content (−0.119). This model explained 11 % of the deviance in k_{iso} compared to the null model. After inclusion of soil pH, the minimal adequate model included the intercept (−4.535) and the additive effects of soil pH (0.4028) and clay content (−0.0017). This model explained 61 % of the deviance in k_{iso} compared to 54 % for the model containing only the intercept (−4.535) and influence of soil pH (0.339).

3.2 Variations induced by NH_4NO_3 addition

The addition of NH_4NO_3 systematically increased available NO_3^- and NH_4^+ and decreased the rate of oxygen isotope exchange, k_{iso}, and soil pH. Available NO_3^- and NH_4^+ in the treated soils that received the NH_4NO_3 addition were respectively 1.9 to 173.6 and 3.7 to 18.8 times greater than in the corresponding untreated soils. Soil pH and k_{iso} were respectively 0.86 to 0.98 and 0.21 to 0.76 times smaller in the soils that received the addition than in the corresponding untreated soils. The addition did not have a systematic influence on microbial biomass, which varied between 0.64 and 1.84 of the magnitude in the corresponding untreated soils.

Individual relationships between pairs of these fractional changes were investigated through Spearman's rank correlation (Table 2). Strong, significant correlations ($p < 0.05$) for variable pairs were found between the fractional changes in k_{iso} and soil pH (Spearman's $\rho = 0.57$), k_{iso} and NO_3^- availability (Spearman's $\rho = -0.84$), and soil pH and NO_3^- availability (Spearman's $\rho = -0.75$). Correlations between all other variable pairings were weaker and non-significant ($p > 0.05$).

https://doi.org/10.5194/soil-2020-44
Preprint. Discussion started: 23 July 2020

Based on AICc and visual inspection of model fit and residuals, the structure of the generalised linear model describing variations in the fractional change in the rate of oxygen isotope exchange, k_{iso}, as the response variable was specified with a betareg error distribution and identity link function (Thomas et al., 2017). The minimal adequate, single term model with this structure included the natural logarithm of the fractional change in NO_3^- availability (−0.499) and an intercept term (1.219). This model predicts the variations in the fractional change in k_{iso} following NH_4NO_3 addition across soils from the 14 sites considered result from a negative relationship with fractional changes in NO_3^- availability (Figure 5). This relationship explained 76 % of the deviance in the fractional change in k_{iso} and the model had an AICc that was 13.2 lower than the next best alternative model which included the fractional change in soil pH and an intercept term.

4 Discussion

This study aimed to investigate the drivers of variations in the rate of oxygen isotope exchange, k_{iso}, between soil water and CO_2 with a view to improving our ability to predict the influence of soils on the $\delta^{18}O$ of atmospheric CO_2 and our understanding of dynamics in the activity of carbonic anhydrases expressed by soil microbial communities. To do so, controlled incubation experiments were conducted with soils sampled from 44 sites across western Eurasia and northeastern Australia in order to estimate k_{iso} and metrics relating to hypothesised controls on this activity. Estimates of k_{iso} for untreated soils ranged from 0.01 to 0.4 s^{-1} (Figure 2 a). In all cases these rates exceeded theoretical uncatalysed rates of oxygen isotope exchange calculated for the incubation conditions (Uchikawa & Zeebe, 2012), which ranged from 0.00008 to 0.008 s^{-1}, indicating the presence of active carbonic anhydrases. These observations, with a median of 0.07 s^{-1}, are in good agreement with a number of previous studies which estimated k_{iso} ranging from 0.03 to 0.15 s^{-1} for sieved soils incubated in the dark (Jones et al., 2017; Sauze et al., 2018, 2017), but are somewhat lower than those reported by Meredith et al. (2019) with a median and range of 0.46 s^{-1} and 0.08 to 0.88 s^{-1}, respectively. These greater k_{iso} are more comparable to those, ranging from 0.01 to 0.75 s^{-1}, reported by Sauze et al. (2017) for soils with well developed algal communities. Direct comparison with field observations is non-trivial because these older studies tend to address soil carbonic anhydrase activity as a range of enhancement factors over a temperature sensitive uncatalysed rate of hydration (Seibt et al., 2006; Wingate et al., 2008, 2009, 2010). However, using the mid-point of the enhancement factors and soil temperatures reported by Wingate et al. (2009), we can estimate that k_{iso} varied between 0.04 and 13 s^{-1} with a median of 0.31 s^{-1} across the seven ecosystems studied. Whether the potential for k_{iso} to be orders of magnitude greater in the field than in incubation studies is an artefact of the sensitivity of the methodology applied to estimate the isotopic composition of the soil water pool from which exchanged CO_2 inherits it's signal (Jones et al., 2017) or a reduction in carbonic anhydrases following the exclusion of potentially active elements of the rhizosphere (Li et al., 2005), phototrophs (Sauze et al., 2017) or fauna in sieved soils remains an unresolved but key question.

https://doi.org/10.5194/soil-2020-44
Preprint. Discussion started: 23 July 2020

We hypothesised that the rate of oxygen isotope exchange, k_{iso}, might be positively correlated with microbial biomass (H1), positively correlated with soil pH (H2) and negatively correlated with NO_3^- availability (H3). We found evidence in support of all three hypotheses with the minimal adequate statistical model explaining variations in k_{iso} observed across untreated soils including all three of these terms (Eq. 6). The model suggests that the positive relationship with soil pH (Figure 3 a), the strongest single predictor of variations in k_{iso}, reinforces the emergent view of soil pH as the principal driver of variations in carbonic anhydrase expression by soil microbial communities (Sauze et al., 2018). Marked increases in k_{iso} under alkaline conditions likely reflects a shift in microbial community towards organisms that express more or more efficient carbonic anhydrases than those found under acidic conditions (Meredith et al., 2019; Sauze et al., 2018, 2017) and the need for organisms to up-regulate carbonic anhydrases expression. This may be required in order to control the transport and availability of CO_2 and bicarbonate in response to the pH dependent speciation of dissolved inorganic carbon (Figure 1 b) as has been observed for both intra- and extra-cellular carbonic anhydrase activity in non-soil settings (Hopkinson et al., 2013; Kaur et al., 2009; Kozliak et al., 1995; Merlin et al., 2003). Similarly, in the positive relationship with microbial biomass (Figure 3 c) we find support for a secondary role for the expected link between the abundance of organisms likely to be expressing carbonic anhydrase and k_{iso} for a given set of biogeochemical conditions (Sauze et al., 2017). Finally, through the negative relationship with NO_3^- availability (Figure 3 b) we show for the first time that k_{iso} in soils is sensitive to dissolved inorganic nitrogen chemistry. Outwith soils, anions including NO_3^- have been shown to inhibit carbonic anhydrase activity by binding with the enzyme (Peltier et al., 1995; Tibell et al., 1984). The fact that this binding and subsequent inhibition of carbonic anhydrase activity has been shown to be more efficient under acidic conditions but have minimal influence at high pH may reflect the role of protonation in this behaviour (Johansson & Forsman, 1993, 1994). Interestingly, the interaction between soil pH and NO_3^- availability identified here, leading to a larger negative influence of NO_3^- availability under acidic conditions (Figure 3 b), is in agreement with this observation. This suggests that the influence of NO_3^- availability on carbonic anhydrases activity is likely minimal in neutral and alkaline soils and the constraints imposed by pH and microbial community size are of greater importance. To better understand the relationship between k_{iso} and soil inorganic nitrogen we conducted an NH_4NO_3 addition experiment. As in other studies, the addition of NH_4NO_3 not only increased the availability of NO_3^- and NH_4^+ but also acted to decrease soil pH and caused non-systematic changes in microbial biomass (Zhang et al., 2017). Reflecting the different magnitudes of these changes, the observed decrease in k_{iso} in soils receiving the addition relative to their untreated counterparts was best explained by the increase in NO_3^- availability (Figure 5). Notably the weak relationship between changes in k_{iso} and NH_4^+ availability identified in this experiment (Table 2) suggests the relationship between these variables across the untreated soils (Table 1) does indeed reflect the pH sensitivity of ammonia speciation rather than a direct causal link. The negative relationship between NO_3^- availability and k_{iso} appears to support the proposed mechanism of carbonic anhydrases inhibition. However, an alternative explanation, invoked to explain reductions in the activity of enzymes involved in nitrogen acquisition following fertilisation (Zhang et al., 2017), may be that carbonic

https://doi.org/10.5194/soil-2020-44
Preprint. Discussion started: 23 July 2020

anhydrases play some role in the soil nitrogen cycle that is alleviated by increases in NO_3^- availability following NH_4NO_3 addition and thus leads to down-regulation of expression (DiMario et al., 2017; Kalloniati et al., 2009; Rigobello-Masini et al., 2006). Indeed, such a function would help explain why the microbial communities in the untreated acidic, higher relative to lower NO_3^- availability soils do not appear to need to compensate for the inhibition of carbonic anhydrases as we might expect from the economic theory of enzyme investment if they are facilitating important metabolic reactions (Burns et al., 2013). Much needed development of our understanding of the intra- and extra-cellular distribution of soil carbonic anhydrases and their relationship to spatial and temporal variations in chemical conditions experienced by the microbial communities that express them are required to confirm the mechanistic link among these observations.

Improvements to our ability to predict the influence of soils on the the $\delta^{18}O$ of atmospheric CO_2 are important in refining the use of this tracer to constrain gross primary production at the ecosystem-scale and above (Wingate et al., 2009; Welp et al., 2011) . The absence of strong patterns with climate or land-cover in this study may well reflect the fact that the temperature and moisture conditions used are unrepresentative of field conditions especially for colder and drier sites (Figure 2 a). Whether or not up-scaling based on such classes is feasible is somewhat unknown (Wingate et al., 2009). However, the data reported here does provide the basis for an empirical approach to predicting the rate of oxygen isotope exchange, k_{iso}, for a given soil (Figure 3). The minimal adequate statistical model described (Eq. 6) was able to provide broadly unbiased predictions of variations observed in k_{iso} across the untreated soils of the 44 sites considered (Figure 4 a). Indeed, broad agreement between predictions of the fractional changes in k_{iso} between untreated and treated, which were not used in model selection, soils following the NH_4NO_3 addition encouragingly suggest that this model could be used to provide reasonable predictions of k_{iso} for other soils (Figure 4 b). More observations from alkaline soils are required to reduce uncertainty found at greater k_{iso} and further validation is required to avoid biased predictions outside of the ranges considered (Figure 3). A significant challenge to using this relationship to predict k_{iso} is likely the availability of suitable pedotransfer functions, particularly for NO_3^- availability and microbial biomass, to estimate patterns in the proposed drivers (Van Looy et al., 2017). Given the interaction between soil pH and NO_3^- availability (Figure 3 a & b), the absence of such data may not seriously compromise predictions for fertilised agricultural soils which are typically not strongly acidic. However, accurately predicting natural spatial and seasonal variability and the influence of future changes in atmospheric NO_3^- deposition (DeForest et al., 2004) may be more problematic. For this reason we considered whether more readily available parameters such as soil texture, carbon content and nitrogen content might provide an alternative basis for empirical predictions of k_{iso} (Van Looy et al., 2017). Relationships between these variables and k_{iso} were relatively weak and could only explain a marginal amount of the observed variability. Considering these properties in combination with soil pH yielded clay content as a secondary significant term potentially reflecting a relatively strong co-correlation (Spearman's $\rho = 0.5$) with NO_3^- availability. Soil pH and clay content may provide an alternative empirical approach to predicting k_{iso} when the availability of soil property data is limited.

https://doi.org/10.5194/soil-2020-44
Preprint. Discussion started: 23 July 2020

Data availability

The underlying research data is part of European Research Council grant no. 338264 and will be made publicly accessible as part of a combined data product for this grant. The data may be requested from the corresponding author by email.

Competing interests

The authors declare that they have no conflict of interest.

Author contributions

Conceptualisation - SJ, AK, JO, SW, AC, LC & LW; Formal analysis – SJ & AK; Funding acquisition – JO & LW; Investigation – SJ, AK, SW & AC; Methodology – SJ, AK, JO & SW; Resources: JO, LC & LW; Writing (original draft) – SJ; Writing (review & editing) – JO, AC & LC.

Acknowledgements

This work was funded by the European Research Council (ERC) under the European Union's Seventh Framework Programme (FP7/2007-2013) grant agreement No. 338264, and the Agence Nationale de la Recherche (ANR) grant number ANR-13-BS06-0005-01. Many thanks to Jorge Curiel-Yuste, Alexandria Correia, Jean-Marc Ourcival, Jukka Pumpanen, Huizhong Zhang, Carmen Emmel, Nina Buchmann, Sabina Keller, Irene Lehner, Anders Lindroth, Andreas Ibrom, Jens Schaarup Sorensen, Dan Yakir, Fulin Yang, Michal Heliasz, Susanne Burri, Penelope Serrano Ortiz, Maria Rosario Moya Jimenez, Jose Luis Vicente, Holger Tulp, Per Marklund, John Marshall, Nils Henriksson, Raquel Lobo de Vale, Lukas Siebicke, Bernard Longdoz, Pascal Courtois, and Katja Klumpp for providing soil from Eurasian sites, Joana Sauze, Ana Gutierrez, and Bastien Frejaville for facilitating analyses made in France, and Jon Lloyd, Paul Nelson, Niels Munksgaard, Jen Whan, Michael Bird, Chris Wurster, and Hilary Stuart-Williams for facilitating analyses made in Australia.

References

Badger, M.: The roles of carbonic anhydrases in photosynthetic CO2 concentrating mechanisms, Photosynthesis Research, 77(2–3), 83, doi:10.1023/A:1025821717773, 2003.

Burns, R. G., DeForest, J. L., Marxsen, J., Sinsabaugh, R. L., Stromberger, M. E., Wallenstein, M. D., Weintraub, M. N. and Zoppini, A.: Soil enzymes in a changing environment: Current knowledge and future directions, Soil Biology and Biochemistry, 58, 216–234, doi:10.1016/j.soilbio.2012.11.009, 2013.

DeForest, J. L., Zak, D. R., Pregitzer, K. S. and Burton, A. J.: Atmospheric Nitrate Deposition, Microbial Community Composition, and Enzyme Activity in Northern Hardwood Forests, Soil Science Society of America Journal, 68(1), 132–138, doi:10.2136/sssaj2004.1320, 2004.

Del Prete, S., Vullo, D., Fisher, G. M., Andrews, K. T., Poulsen, S.-A., Capasso, C. and Supuran, C. T.: Discovery of a new family of carbonic anhydrases in the malaria pathogen Plasmodium falciparum—The η-carbonic anhydrases, Bioorganic & Medicinal Chemistry Letters, 24(18), 4389–4396, doi:10.1016/j.bmcl.2014.08.015, 2014.

DiMario, R. J., Clayton, H., Mukherjee, A., Ludwig, M. and Moroney, J. V.: Plant Carbonic Anhydrases: Structures, Locations, Evolution, and Physiological Roles, Mol Plant, 10(1), 30–46, doi:10.1016/j.molp.2016.09.001, 2017.

Francey, R. J. and Tans, P. P.: Latitudinal variation in oxygen-18 of atmospheric CO2, Nature, 327(6122), 495–497, doi:10.1038/327495a0, 1987.

Gillon, J. and Yakir, D.: Influence of Carbonic Anhydrase Activity in Terrestrial Vegetation on the 18O Content of Atmospheric CO2, Science, 291(5513), 2584–2587, doi:10.1126/science.1056374, 2001.

Haney, R. L. and Haney, E. B.: Simple and Rapid Laboratory Method for Rewetting Dry Soil for Incubations, Communications in Soil Science and Plant Analysis, 41(12), 1493–1501, doi:10.1080/00103624.2010.482171, 2010.

Hopkinson, B. M., Meile, C. and Shen, C.: Quantification of Extracellular Carbonic Anhydrase Activity in Two Marine Diatoms and Investigation of Its Role, Plant Physiol., 162(2), 1142–1152, doi:10.1104/pp.113.217737, 2013.

Johansson, I.-M. and Forsman, C.: Kinetic studies of pea carbonic anhydrase, European Journal of Biochemistry, 218(2), 439–446, doi:10.1111/j.1432-1033.1993.tb18394.x, 1993.

Johansson, I.-M. and Forsman, C.: Solvent Hydrogen Isotope Effects and Anion Inhibition of CO2 Hydration Catalysed by Carbonic Anhydrase from Pisum sativum, European Journal of Biochemistry, 224(3), 901–907, doi:10.1111/j.1432-1033.1994.00901.x, 1994.

Jones, S. P., Ogée, J., Sauze, J., Wohl, S., Saavedra, N., Fernández-Prado, N., Maire, J., Launois, T., Bosc, A. and Wingate, L.: Non-destructive estimates of soil carbonic anhydrase activity and associated soil water oxygen isotope composition, Hydrology and Earth System Sciences, 21(12), 6363–6377, doi:https://doi.org/10.5194/hess-21-6363-2017, 2017.

Kaisermann, A., Ogée, J., Sauze, J., Wohl, S., Jones, S. P., Gutierrez, A. and Wingate, L.: Disentangling the rates of carbonyl sulfide (COS) production and consumption and their dependency on soil properties across biomes and land use types, Atmospheric Chemistry and Physics, 18(13), 9425–9440, doi:https://doi.org/10.5194/acp-18-9425-2018, 2018a.

Kaisermann, A., Jones, S. P., Wohl, S., Ogée, J. and Wingate, L.: Nitrogen Fertilization Reduces the Capacity of Soils to Take up Atmospheric Carbonyl Sulphide, Soil Systems, 2(4), 62, doi:10.3390/soilsystems2040062, 2018b.

Kalloniati, C., Tsikou, D., Lampiri, V., Fotelli, M. N., Rennenberg, H., Chatzipavlidis, I., Fasseas, C., Katinakis, P. and Flemetakis, E.: Characterization of a Mesorhizobium loti α-Type Carbonic Anhydrase and Its Role in Symbiotic Nitrogen Fixation, Journal of Bacteriology, 191(8), 2593–2600, doi:10.1128/JB.01456-08, 2009.

Kaur, S., Mishra, M. N. and Tripathi, A. K.: Regulation of expression and biochemical characterization of a β-class carbonic anhydrase from the plant growth-promoting rhizobacterium, Azospirillum brasilense Sp7, FEMS Microbiology Letters, 299(2), 149–158, doi:10.1111/j.1574-6968.2009.01736.x, 2009.

Kottek, M., Grieser, J., Beck, C., Rudolf, B. and Rubel, F.: World Map of the Köppen-Geiger climate classification updated, metz, 15(3), 259–263, doi:10.1127/0941-2948/2006/0130, 2006.

Kozliak, E. I., Fuchs, J. A., Guilloton, M. B. and Anderson, P. M.: Role of bicarbonate/CO2 in the inhibition of Escherichia coli growth by cyanate., J. Bacteriol., 177(11), 3213–3219, doi:10.1128/jb.177.11.3213-3219.1995, 1995.

Krulwich, T. A., Sachs, G. and Padan, E.: Molecular aspects of bacterial pH sensing and homeostasis, Nature Reviews Microbiology, 9(5), 330, doi:10.1038/nrmicro2549, 2011.

Li, W., Yu, L., Yuan, D., Wu, Y. and Zeng, X.: A study of the activity and ecological significance of carbonic anhydrase from soil and its microbes from different karst ecosystems of Southwest China, Plant Soil, 272(1–2), 133–141, doi:10.1007/s11104-004-4335-9, 2005.

Linn, D. M. and Doran, J. W.: Effect of Water-Filled Pore Space on Carbon Dioxide and Nitrous Oxide Production in Tilled and Nontilled Soils, Soil Science Society of America Journal, 48(6), 1267–1272, doi:10.2136/sssaj1984.03615995004800060013x, 1984.

Massman, W. J.: A review of the molecular diffusivities of H2O, CO2, CH4, CO, O3, SO2, NH3, N2O, NO, and NO2 in air, O2 and N2 near STP, Atmospheric Environment, 32(6), 1111–1127, doi:10.1016/S1352-2310(97)00391-9, 1998.

Meredith, L. K., Ogée, J., Boye, K., Singer, E., Wingate, L., Sperber, C. von, Sengupta, A., Whelan, M., Pang, E., Keiluweit, M., Brüggemann, N., Berry, J. A. and Welander, P. V.: Soil exchange rates of COS and CO 18 O differ with the diversity of microbial communities and their carbonic anhydrase enzymes, The ISME Journal, 13(2), 290, doi:10.1038/s41396-018-0270-2, 2019.

Merlin, C., Masters, M., McAteer, S. and Coulson, A.: Why Is Carbonic Anhydrase Essential to Escherichia coli?, J. Bacteriol., 185(21), 6415–6424, doi:10.1128/JB.185.21.6415-6424.2003, 2003.

Miller, J. B., Yakir, D., White, J. W. C. and Tans, P. P.: Measurement of 18O/16O in the soil-atmosphere CO2 flux, Global Biogeochem. Cycles, 13(3), 761–774, doi:10.1029/1999GB900028, 1999.

Mills, G. A. and Urey, H. C.: The Kinetics of Isotopic Exchange between Carbon Dioxide, Bicarbonate Ion, Carbonate Ion and Water1, J. Am. Chem. Soc., 62(5), 1019–1026, doi:10.1021/ja01862a010, 1940.

Moldrup, P., Olesen, T., Komatsu, T., Yoshikawa, S., Schjønning, P. and Rolston, D.: Modeling diffusion and reaction in soils: X. A unifying model for solute and gas diffusivity in unsaturated soil, Soil Science, 168(5), 321–337, 2003.

Peltier, G., Cournac, L., Despax, V., Dimon, B., Fina, L., Genty, B. and Rumeau, D.: Carbonic anhydrase activity in leaves as measured in vivo by<Superscript>18</Superscript>O exchange between carbon dioxide and water, Planta, 196(4), 732–739, doi:10.1007/BF01106768, 1995.

R Core Team: R: A Language and Environment for Statistical Computing, R Foundation for Statistical Computing, Vienna, Austria. [online] Available from: https://www.R-project.org/, 2019.

Ramirez, K. S., Craine, J. M. and Fierer, N.: Consistent effects of nitrogen amendments on soil microbial communities and processes across biomes, Global Change Biology, 18(6), 1918–1927, doi:10.1111/j.1365-2486.2012.02639.x, 2012.

Rigobello-Masini, M., Masini, J. C. and Aidar, E.: The profiles of nitrate reductase and carbonic anhydrase activity in batch cultivation of the marine microalgae Tetraselmis gracilis growing under different aeration conditions, FEMS Microbiology Ecology, 57(1), 18–25, doi:10.1111/j.1574-6941.2006.00106.x, 2006.

Rowlett, R. S., Tu, C., McKay, M. M., Preiss, J. R., Loomis, R. J., Hicks, K. A., Marchione, R. J., Strong, J. A., Donovan Jr., G. S. and Chamberlin, J. E.: Kinetic characterization of wild-type and proton transfer-impaired variants of β-carbonic anhydrase from Arabidopsis thaliana, Archives of Biochemistry and Biophysics, 404(2), 197–209, doi:10.1016/S0003-9861(02)00243-6, 2002.

Rubel, F., Brugger, K., Haslinger, K. and Auer, I.: The climate of the European Alps: Shift of very high resolution Köppen-Geiger climate zones 1800–2100, metz, 26(2), 115–125, doi:10.1127/metz/2016/0816, 2017.

Sauze, J., Ogée, J., Maron, P.-A., Crouzet, O., Nowak, V., Wohl, S., Kaisermann, A., Jones, S. P. and Wingate, L.: The interaction of soil phototrophs and fungi with pH and their impact on soil CO2, CO18O and OCS exchange, Soil Biology and Biochemistry, 115(Supplement C), 371–382, doi:10.1016/j.soilbio.2017.09.009, 2017.

Sauze, J., Jones, S. P., Wingate, L., Wohl, S. and Ogée, J.: The role of soil pH on soil carbonic anhydrase activity, Biogeosciences, 15(2), 597–612, doi:10.5194/bg-15-597-2018, 2018.

Seibt, U., Wingate, L., Lloyd, J. and Berry, J. A.: Diurnally variable δ18O signatures of soil CO2 fluxes indicate carbonic anhydrase activity in a forest soil, J. Geophys. Res., 111(G4), G04005, doi:10.1029/2006JG000177, 2006.

Smith, K. S. and Ferry, J. G.: Prokaryotic carbonic anhydrases, FEMS Microbiology Reviews, 24(4), 335–366, doi:10.1111/j.1574-6976.2000.tb00546.x, 2000.

Tans, P. P.: Oxygen isotopic equilibrium between carbon dioxide and water in soils, Tellus B, 50(2), doi:10.3402/tellusb.v50i2.16094, 1998.

Thomas, R., Lello, J., Medeiros, R., Pollard, A., Robinson, P., Seward, A., Smith, J., Vafidis, J. and Vaughan, I.: Data Analysis with R Statistical Software: A guidebook for Scientists, Eco-explore, Caerphilly, Wales., 2017.

Tibell, L., Forsman, C., Simonsson, I. and Lindskog, S.: Anion Inhibition of CO2 hydration catalyzed by human carbonic anhydrase II: Mechanistic implications, Biochimica et Biophysica Acta (BBA) - Protein Structure and Molecular Enzymology, 789(3), 302–310, doi:10.1016/0167-4838(84)90186-9, 1984.

Uchikawa, J. and Zeebe, R. E.: The effect of carbonic anhydrase on the kinetics and equilibrium of the oxygen isotope exchange in the CO2–H2O system: Implications for δ18O vital effects in biogenic carbonates, Geochimica et Cosmochimica Acta, 95, 15–34, doi:10.1016/j.gca.2012.07.022, 2012.

Van Looy, K., Bouma, J., Herbst, M., Koestel, J., Minasny, B., Mishra, U., Montzka, C., Nemes, A., Pachepsky, Y. A., Padarian, J., Schaap, M. G., Tóth, B., Verhoef, A., Vanderborght, J., Ploeg, M. J. van der, Weihermüller, L., Zacharias, S., Zhang, Y. and Vereecken, H.: Pedotransfer Functions in Earth System Science: Challenges and Perspectives, Reviews of Geophysics, 55(4), 1199–1256, doi:10.1002/2017RG000581, 2017.

Weiss, R. F.: Carbon dioxide in water and seawater: the solubility of a non-ideal gas, Marine Chemistry, 2(3), 203–215, doi:10.1016/0304-4203(74)90015-2, 1974.

https://doi.org/10.5194/soil-2020-44
Preprint. Discussion started: 23 July 2020

Wingate, L., Seibt, U., Maseyk, K., Ogée, J., Almeida, P., Yakir, D., Pereira, J. S. and Mencuccini, M.: Evaporation and carbonic anhydrase activity recorded in oxygen isotope signatures of net CO2 fluxes from a Mediterranean soil, Global Change Biology, 14(9), 2178–2193, doi:10.1111/j.1365-2486.2008.01635.x, 2008.

Wingate, L., Ogée, J., Cuntz, M., Genty, B., Reiter, I., Seibt, U., Yakir, D., Maseyk, K., Pendall, E. G., Barbour, M. M., Mortazavi, B., Burlett, R., Peylin, P., Miller, J., Mencuccini, M., Shim, J. H., Hunt, J. and Grace, J.: The impact of soil microorganisms on the global budget of δ18O in atmospheric CO2, PNAS, 106(52), 22411–22415, doi:10.1073/pnas.0905210106, 2009.

Wingate, L., Ogée, J., Burlett, R. and Bosc, A.: Strong seasonal disequilibrium measured between the oxygen isotope signals of leaf and soil CO2 exchange, Global Change Biology, 16(11), 3048–3064, doi:10.1111/j.1365-2486.2010.02186.x, 2010.

Zhang, C., Zhang, X.-Y., Zou, H.-T., Kou, L., Yang, Y., Wen, X.-F., Li, S.-G., Wang, H.-M. and Sun, X.-M.: Contrasting effects of ammonium and nitrate additions on the biomass of soil microbial communities and enzyme activities in subtropical China, Biogeosciences, 14(20), 4815–4827, doi:https://doi.org/10.5194/bg-14-4815-2017, 2017.

https://doi.org/10.5194/soil-2020-44
Preprint. Discussion started: 23 July 2020

Tables

Table 1: Spearman's rank correlation coefficients (ρ) for relationships between site mean oxygen isotope exchange rate (k_{iso}), soil pH, microbial biomass (MB), NO_3^- availability and NH_4^+ availability measured in untreated soils (n = 44). * indicates $p < 0.05$ and ** indicates $p < 0.01$.

	k_{iso}	pH	MB	NO_3^-	NH_4^+
k_{iso}	-	0.58**	0.16	−0.25	−0.62**
pH	0.58**	-	−0.27	0.01	−0.73**
MB	0.16	−0.27	-	0.29	0.05
NO_3−	−0.25	0.01	0.29	-	0.11
NH_4^+	−0.62**	−0.73**	0.05	0.11	-

Table 2: Spearman's rank correlation coefficients (ρ) for relationships between changes in the ratio of mean rate of oxygen isotope exchange (k_{iso}), soil pH, microbial biomass (MB), NO_3^- availability and NH4+ availability between soils receiving a NH_4NO_3 addition and that of the corresponding untreated soils (n = 14). * indicates $p < 0.05$ and ** indicates $p < 0.01$.

	k_{iso}	pH	MB	NO_3^-	NH_4^+
k_{iso}	-	0.57*	0.37	−0.84**	0.14
pH	0.57*	-	0.22	−0.75**	0.02
MB	0.37	0.22	-	−0.32	0.18
NO_3−	−0.84**	−0.75**	−0.32	-	0.09
NH_4^+	0.14	0.02	0.18	0.09	-

https://doi.org/10.5194/soil-2020-44
Preprint. Discussion started: 23 July 2020

Figures

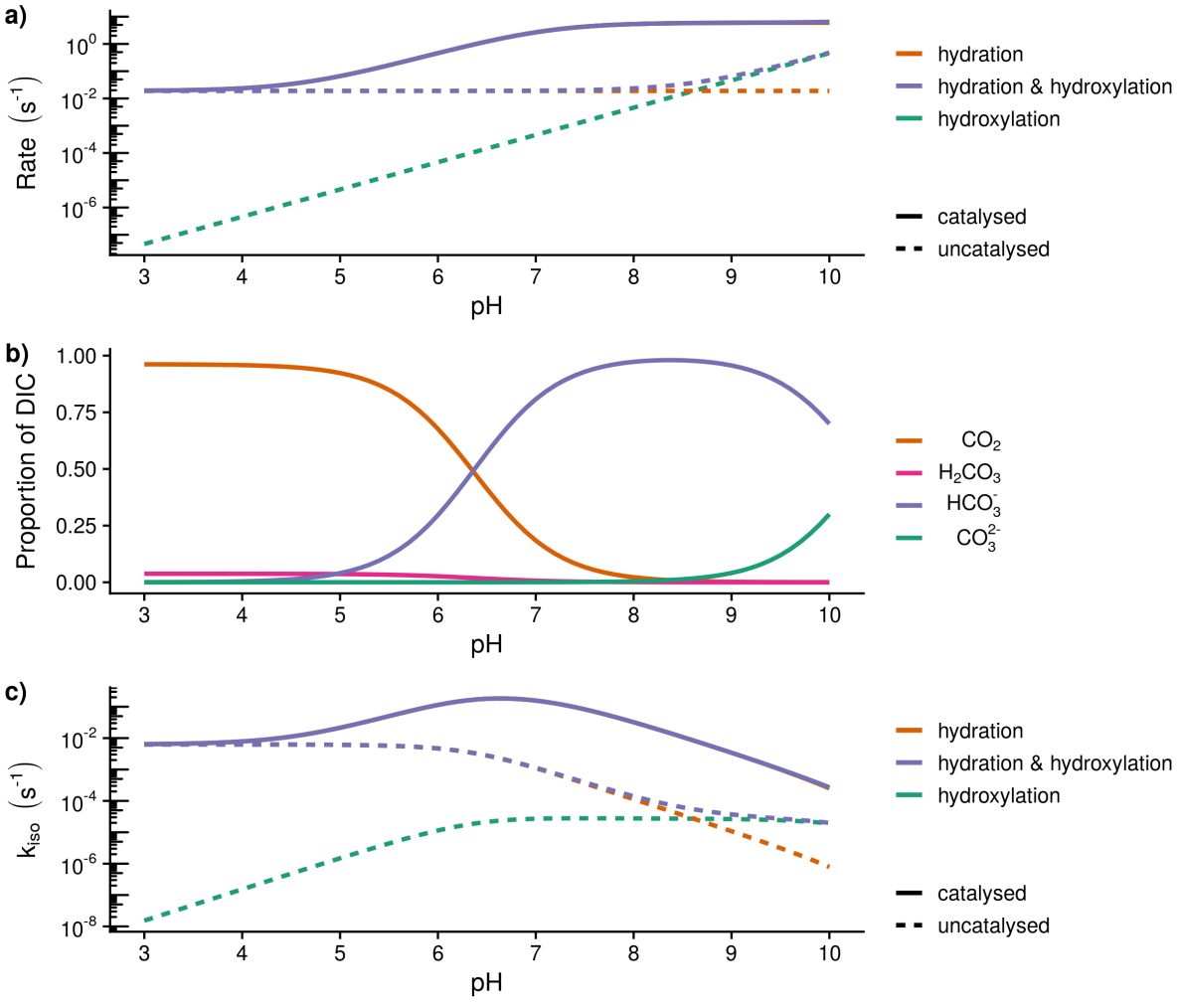

Figure 1: Theoretical calculations of the expected relationship between the rate of hydration (k_h) and hydroxylation reactions, the speciation of dissolved organic carbon (DIC) and the rate of oxygen isotope exchange (k_{iso}): a) expected variations in the rate of hydration (k_h) and hydroxylation reactions with pH at 21 °C calculated following Uchikawa & Zeebe (2012) and Sauze et al. (2018). Dashed lines indicate uncatalysed rates whilst solid lines include the presence of 200 nM of carbonic anhyrdrase with a k_{cat}/k_m = 3 x 10^7 M s^{-1} and a pka of 7.1. The catalysed rate of hydration decreases under acidic conditions as high proton concentrations limit enzyme regeneration, b) Speciation of dissolved organic carbon (DIC) calculated from rate constants at 21 °C, c) Expected variations in the rate of isotope exchange (k_{iso}) with pH calculated as in the first panel (a). The rate of exchange is limited by enzyme regeneration under acidic conditions and the availability of CO_2 under alkaline conditions.

https://doi.org/10.5194/soil-2020-44
Preprint. Discussion started: 23 July 2020

645

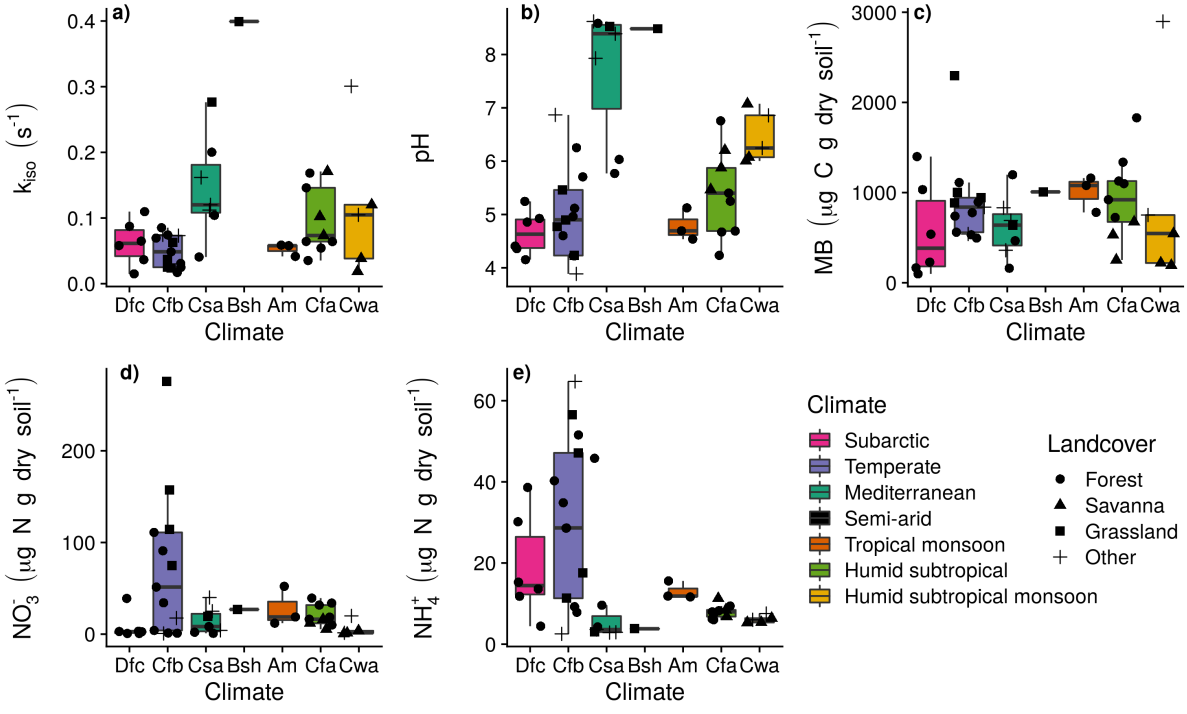

Figure 2: Measurement summaries of mean untreated soils by Köppen-Geiger climatic zone of the sampling site. The 27 sites in western Eurasian (EUR) were within Subartctic (Dfc; n= 6), Temperate oceanic (Cfb; n= 13), Hot-summer Mediterraean (Csa; n = 7) and Hot semi-arid (Bsh; n = 1) climate zones and the 17 sites in north Queensland, Australia (AUS) were within Tropical monsoon (Am; n = 3), Humid subtropical (Cfa; n = 9) and Monsoon-influenced humid subtropical (Cwa; n= 5) climate zones. Box lower, middle and upper hinges respectively indicate 0.25, 0.5 and 0.75 quantiles. Over-plotted points are the associated site means (n=2 or 3) with shape indicating land-cover: a) k_{iso}, b) pH, c) microbial biomass (MB), d) NO_3^- availability, and d) NH_4^+ availability.

https://doi.org/10.5194/soil-2020-44
Preprint. Discussion started: 23 July 2020

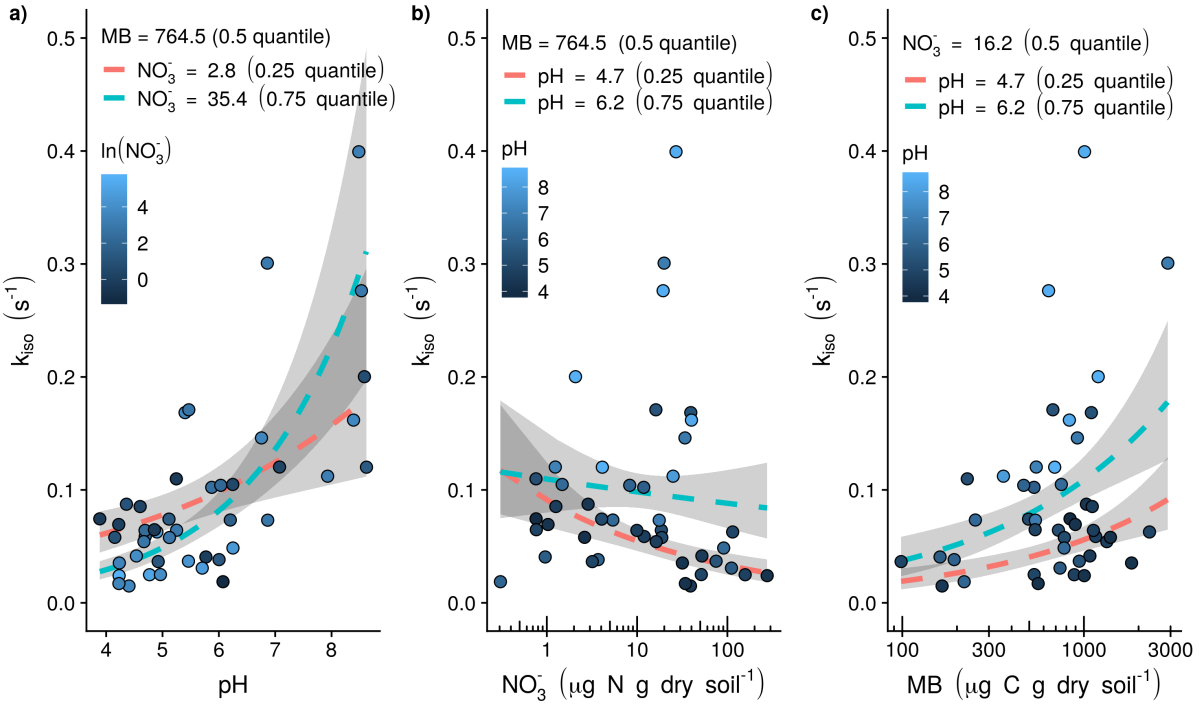

Figure 3: Observed (points) and modelled relationships following Eq. 6 (dashed lines) between the rate of oxygen isotope exchange (k_{iso}) and soil pH, NO_3^- availability and microbial biomass (MB): a) the positive relationship between k_{iso} and soil pH with model response as a function of the shown range in soil pH calculated with median microbial biomass and lower quartile (red dashed line) and upper quartile (blue dashed line) NO_3^- availability, b) the negative relationship between k_{iso} and NO_3^- availability with model response as a function of the shown range in NO_3^- availability calculated with median microbial biomass and lower quartile (red dashed line) and upper quartile (blue dashed line) soil pH, and c) the positive relationship between k_{iso} and microbial biomass with the model response as a function of the shown range in microbial biomass calculated with median soil pH and NO_3^- availability (red dashed line). Grey shaded areas indicate the 95 % confidence intervals associated with model fits.

https://doi.org/10.5194/soil-2020-44
Preprint. Discussion started: 23 July 2020

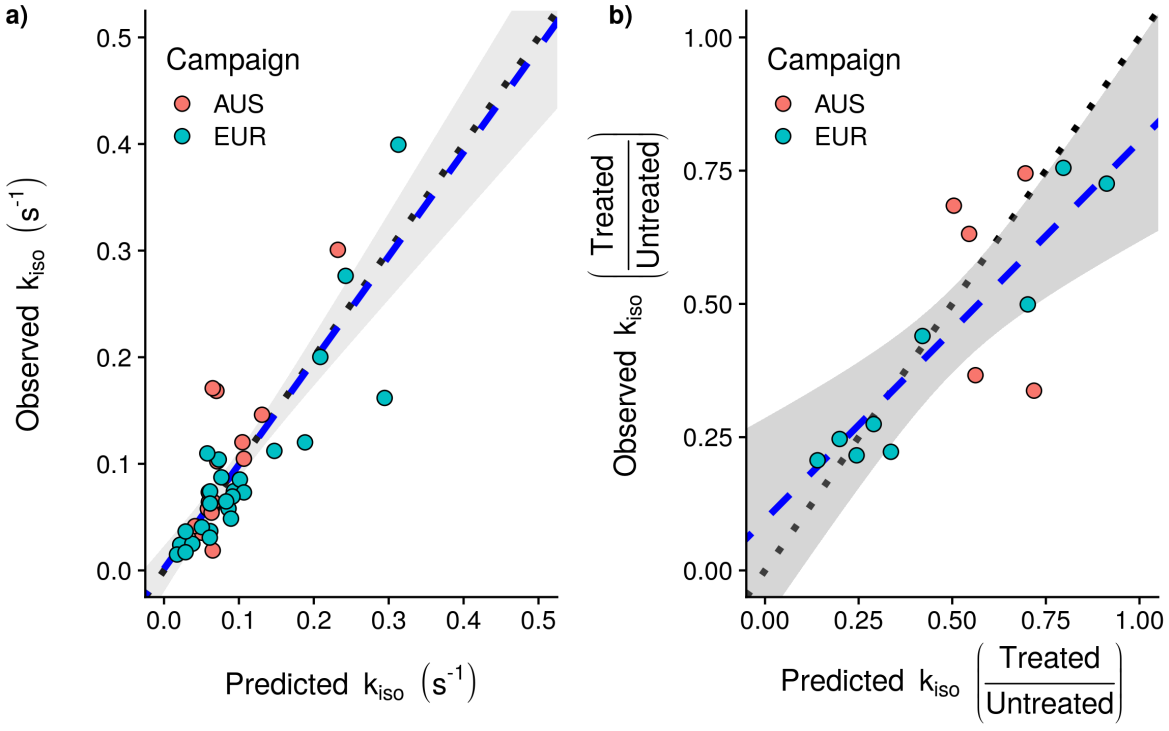

Figure 4: Rates of oxygen isotope exchange (k_{iso}) predicted by the minimal adequate model statistical model identified (Eq. 6): a) model predictions for the 44 untreated soils against the observations for these soils used in model fitting and b) predicted fractional changes in k_{iso} between treated and untreated soils against the changes observed following NH_4NO_3 addition. Plotted points indicate individual sites with the associate sampling campaign indicated by colour (EUR: blue, n = 9; AUS: red, n = 5), dotted lines indicate the 1:1 line and dashed blue lines indicate linear relationships between predicted and observed values with a shaded 95 % confidence interval.

https://doi.org/10.5194/soil-2020-44
Preprint. Discussion started: 23 July 2020

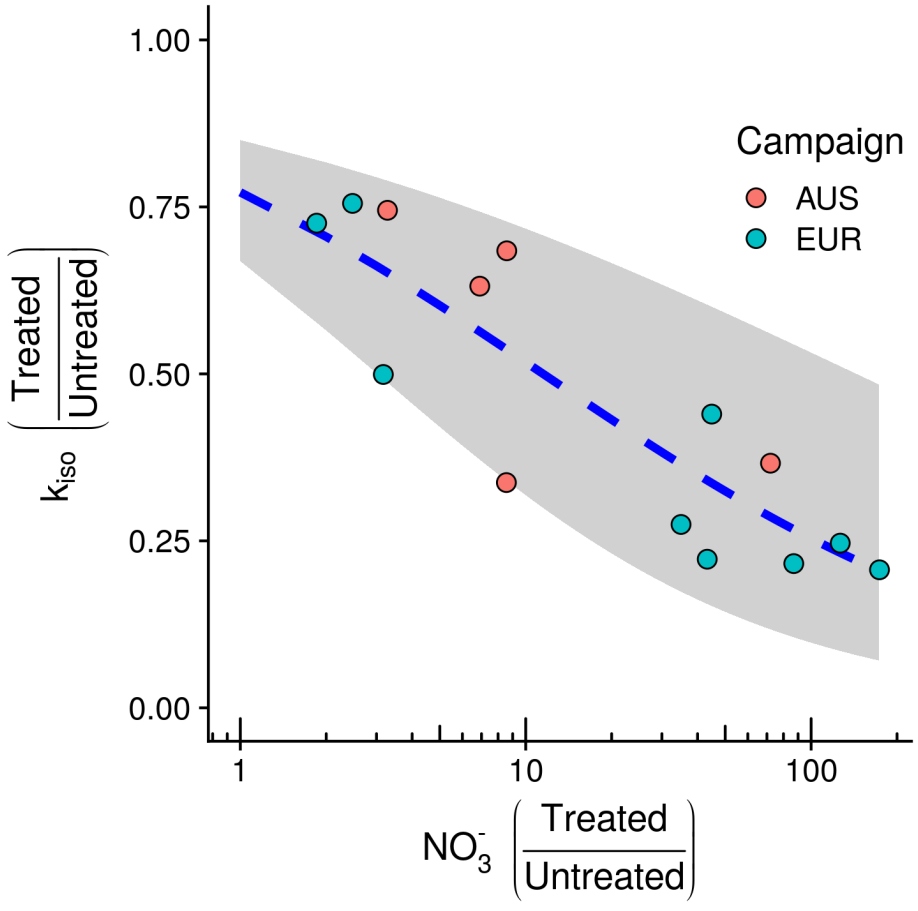

Figure 5: Observed negative relationship between the fractional change in the rate of oxygen isotope exchange (k_{iso}) and the fractional change in NO_3^- availability between treated and untreated soils following NH_4NO_3 addition for the 14 sites considered. Plotted points indicate the change for individual sites with the associate sampling campaign indicated by colour (EUR: blue, n= 9; AUS: red, n = 5). On the y-axis, quotients below 1 indicate k_{iso} in soils receiving the treatment decreased relative to corresponding untreated soils for each site. On the x-axis, quotients above 1 indicate NO_3^- availability in soils receiving the treatment increased relative to corresponding untreated soils for each site. The blue dashed line shows the fit of the minimal adequate generalised linear model describing the change in k_{iso} with 95 % confidence intervals shaded in grey.